DALTON
FULL PAPER

Cycloheptatriene: a new versatile co-ordination ligand. Synthesis and structural characterization of $[Ru_6C(CO)_{17}]$ derivatives

Dario Braga,*[a] Fabrizia Grepioni,[a] Laura Scaccianoce[b] and Brian F. G. Johnson*[b]

[a] *Dipartimento di Chimica G. Ciamician, Università di Bologna, Via Selmi 2, 40126 Bologna, Italy*
[b] *Department of Chemistry, The University of Cambridge, Lensfield Road, Cambridge, UK CB2 1EW*

The reaction of $[Ru_6C(CO)_{17}]$ and cycloheptatriene (CHT) gives rise to the formation of several products which have been fully characterized in solution and by single-crystal X-ray diffraction as $[Ru_6C(CO)_{15}(ENBD)]$ **1** (ENBD = ethylenenorbornadiene), $[Ru_6C(CO)_{14}(C_7H_8)]$ **2** and $[Ru_6C(CO)_{11}(\eta^5\text{-}C_7H_9)(\mu_3\text{-}\eta^2\text{:}\eta^2\text{:}\eta^3\text{-}C_7H_7)]$ **3**. Compounds **2** and **3** provide an example of the co-ordinative variability of carbocyclic rings based on the C_7-frame. The ligand in **1** contains nine carbon atoms and is formed from C_7H_9 by an unknown process. The CHT molecule has also been observed to convert to toluene through a ring contraction activated by the cluster to form the known compound $[Ru_6C(CO)_{14}(\eta^6\text{-}C_6H_5CH_3)]$ **4**.

The interaction of carbocycles with transition-metal clusters has been extensively studied.[1] Metal–arene clusters are particularly interesting because of their potential involvement in catalytic reactions, and as models for chemisorption and heterogeneous catalysis.[2] In fact, on co-ordination to a cluster unit, the organic ligand has a reactivity different to that of the unco-ordinated ligand, and this is especially true for organic π-electron systems. It has been found that the metal clusters provide potential analogues for the study of the structure and reactivity of organic molecules on metal surfaces within heterogeneous catalytic systems, especially when the metals form a metal–metal bonding network. There are two factors to be considered in a catalytic reaction:[3] the reduction of the activation energy of the reaction, and the selectivity that a catalyst may provide.[4] However, the characterization of a molecular species chemisorbed on the surface of a heterogeneous catalyst is far more difficult than that of a molecule co-ordinated to a metal ion. Whilst in the latter case single-crystal X-ray diffraction is the method of choice, other techniques, for example low-energy electron diffraction (LEED) and Auger spectroscopy,[5] are utilized for the characterization of surfaces.

As stated previously, metal clusters are potentially simple models of surfaces in chemisorption and catalytic processes. Being discrete molecular entities soluble in non-reactive solvents, metal clusters provide all the characteristics of simple mononuclear homogeneous catalysts for the definition of structure, stereochemistry, dynamic chemistry (ligand mobility), and the mechanistic details of catalytic chemistry.

Transition-metal clusters are also available to activate both C–H and C–C bonds. This behaviour is significant, especially in the industrial context. It is well known, for example, that the Pt(111) surface acts as a catalyst in reactions such as the formation of benzene from cyclic C_6 hydrocarbons such as cyclohexane, cyclohexene and cyclohexadiene, through the absorption of these molecules on its surface. In this case the reaction is a dehydrogenation.[6] Transition-metal clusters react similarly with these ring systems, showing once again their similarity to the metal surface. Other common processes observed with clusters are the contraction of C_6 and C_8 rings to C_5 (cyclopentadienyl) derivatives (C_8 rings may also contract to C_6 rings). Similar products may also be obtained when C_6 and C_8 rings are chemisorbed on a Pt(111) surface, or on supported Group VIII metals (*e.g.* Ni, Pd or Pt) and metal sulfide (*e.g.* MoS_2, WS_2, Co–Mo–S/Al_2O_3) catalysts. In cluster chemistry it is known that these reactions are complex because of the change in cluster nuclearity, the different CO bonding modes available and, finally, the number of products isolated. Thus, the mechanism of these reactions is unclear. However, it is believed that the contraction process occurs whilst the ligand is co-ordinated to the metal unit and that the dehydrogenation takes place subsequently. This mechanistic pathway is believed to occur in reactions involving both C_6 and C_8 rings. It is important to note that as the cluster increases in nuclearity from three to six, different mechanisms may operate.[7]

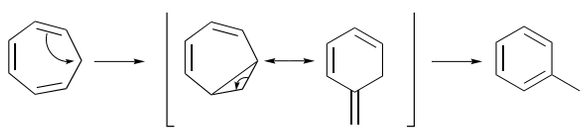

Scheme 1 Mechanism of the ring contraction from CHT to toluene

In this current study, we have extended our investigation of the chemistry and structures of metal–arene cluster derivatives of $[Ru_6C(CO)_{17}]$[8] to that of the products of the reaction with CHT (cycloheptatriene). We have found that CHT is remarkably adaptable and able to adopt a variety of bonding bonds, and that it is also easily transformed *via* ring-contraction into toluene or *via* condensation through bicyclic C_9 systems.

Results and Discussion

The reaction of $[Ru_6C(CO)_{17}]$ and CHT (cycloheptatriene) gives rise to several products which have been fully characterized by single-crystal X-ray diffraction: $[Ru_6C(CO)_{15}(ENBD)]$ **1** [ENBD = ethylenenorbornadiene = 1-(ethenyl)bicyclo[2.2.1]hepta-2,5-diene], $[Ru_6C(CO)_{14}(C_7H_8)]$ **2** and $[Ru_6C(CO)_{11}(\eta^5\text{-}C_7H_9)(\mu_3\text{-}\eta^2\text{:}\eta^2\text{:}\eta^3\text{-}C_7H_7)]$ **3**. In one case the CHT molecule converted into toluene apparently through a ring contraction activated by the cluster to give the toluene derivative $[Ru_6C(CO)_{14}(\eta^6\text{-}C_6H_5CH_3)]$ **4** which is already known.[9] The mechanism of this contraction has not been established. However, ring contraction aided by interaction with transition-metal ions is a well recorded phenomenon, and in this case we believe that contraction may follow the course outlined in Scheme 1. The formation of the bicyclic compound **1** as the major product of the reaction is difficult to explain. Certainly it does not appear to be an intermediate in the formation of products **2** and **3** and the source of the additional C_2 fragment is unknown.

Table 1 The Ru–Ru bond lengths (Å) for cluster **1a**, **1b**, **2** and **3**

	1a	1b	2	3
Ru(1)–Ru(2)	2.813(2)		2.843(2)	2.906(2)
Ru(1)–Ru(3)	3.020(1)		2.885(2)	2.882(2)
Ru(1)–Ru(4)	2.969(1)		2.911(2)	2.852(1)
Ru(1)–Ru(5)	2.969(2)		2.875(2)	2.854(3)
Ru(2)–Ru(3)	2.912(2)		2.970(2)	2.790(2)
Ru(2)–Ru(4)				2.897(1)
Ru(2)–Ru(5)	2.932(1)		2.964(2)	2.968(3)
Ru(2)–Ru(6)	2.874(1)		2.907(2)	
Ru(3)–Ru(4)	2.879(1)		2.832(2)	
Ru(3)–Ru(5)				2.949(1)
Ru(3)–Ru(6)	2.809(2)		2.941(2)	3.014(2)
Ru(4)–Ru(5)	2.866(2)		2.829(2)	2.925(2)
Ru(4)–Ru(6)	2.956(2)		2.896(2)	2.937(2)
Ru(5)–Ru(6)	2.804(1)		2.851(2)	2.861(2)
Ru(7)–Ru(8)		3.036(1)		
Ru(7)–Ru(9)		2.932(2)		
Ru(7)–Ru(10)		2.970(2)		
Ru(7)–Ru(11)		2.827(1)		
Ru(8)–Ru(9)		2.867(2)		
Ru(8)–Ru(11)		2.914(1)		
Ru(8)–Ru(12)		2.810(2)		
Ru(9)–Ru(10)		2.867(1)		
Ru(9)–Ru(12)		2.919(2)		
Ru(10)–Ru(11)		2.930(1)		
Ru(10)–Ru(12)		2.804(1)		
Ru(11)–Ru(12)		2.910(2)		

Table 2 The C–C bond lengths (Å) for cluster **1a**, **1b**, **2** and **3**

	1a	1b	2	3
C(1)–C(2)	1.39(2)			
C(1)–C(6)	1.54(2)			
C(1)–C(7)				
C(2)–C(3)	1.56(2)			
C(3)–C(4)	1.54(2)			
C(3)–C(7)	1.53(2)			
C(4)–C(5)	1.43(2)			
C(5)–C(6)	1.54(2)			
C(6)–C(7)	1.54(2)			
C(6)–C(8)	1.47(2)			
C(8)–C(9)	1.33(2)			
C(10)–C(11)		1.40(2)		
C(10)–C(15)		1.53(2)		
C(11)–C(12)		1.52(2)		
C(12)–C(13)		1.53(2)		
C(12)–C(16)		1.54(2)		
C(13)–C(14)		1.41(2)		1.389(8)
C(13)–C(19)				1.432(8)
C(14)–C(15)		1.54(2)		1.439(8)
C(15)–C(16)		1.56(2)	1.45(2)	1.403(8)
C(15)–C(17)			1.50(2)	
C(15)–C(21)			1.40(2)	
C(16)–C(17)			1.42(2)	1.437(8)
C(17)–C(18)		1.27(2)	1.42(2)	1.398(8)
C(18)–C(19)			1.41(2)	1.454(8)
C(19)–C(20)			1.51(2)	
C(20)–C(21)			1.51(2)	1.396(9)
C(20)–C(26)				1.419(9)
C(21)–C(22)				1.428(8)
C(22)–C(23)				1.512(8)
C(23)–C(24)				1.49(1)
C(24)–C(25)				1.513(9)
C(25)–C(26)				1.414(8)

Table 3 Selected angles (°) for clusters **1a**, **1b**, **2** and **3**

	1a	1b	2	3
C(2)–C(1)–C(6)	108(1)			
C(7)–C(1)–C(2)				
C(1)–C(2)–C(3)	105(1)			
C(7)–C(3)–C(4)	102(1)			
C(7)–C(3)–C(2)	100(1)			
C(4)–C(3)–C(2)	100(1)			
C(5)–C(4)–C(3)	105(1)			
C(4)–C(5)–C(6)	107(1)			
C(8)–C(6)–C(7)	121(1)			
C(8)–C(6)–C(1)	117(1)			
C(7)–C(6)–C(1)	100.5(9)			
C(8)–C(6)–C(5)	117(1)			
C(7)–C(6)–C(5)	100.7(9)			
C(1)–C(6)–C(5)	96.4(9)			
C(3)–C(7)–C(6)	95.8(9)			
C(6)–C(7)–C(1)				
C(9)–C(8)–C(6)	125(1)			
C(11)–C(10)–C(15)		106(1)		
C(10)–C(11)–C(12)		107(1)		
C(11)–C(12)–C(13)		98(1)		
C(11)–C(12)–C(16)		102(1)		
C(13)–C(12)–C(16)		100(1)		
C(14)–C(13)–C(12)		108(1)		
C(13)–C(14)–C(15)		105(1)		128.4(5)
C(17)–C(15)–C(10)		120(1)		
C(17)–C(15)–C(14)		117(1)		
C(10)–C(15)–C(14)		98.1(9)		
C(17)–C(15)–C(16)		116(1)		
C(10)–C(15)–C(16)		102(1)		
C(14)–C(15)–C(16)		101(1)		129.4(5)
C(12)–C(16)–C(15)		94(1)		
C(18)–C(17)–C(15)		127(2)		
C(21)–C(15)–C(16)				
C(15)–C(16)–C(17)			127(1)	128.6(5)
C(18)–C(17)–C(16)			128(1)	128.5(5)
C(19)–C(18)–C(17)			129(1)	124.0(5)
C(18)–C(19)–C(20)			129(1)	
C(21)–C(20)–C(19)			124(1)	
C(15)–C(21)–C(20)			118(1)	
C(14)–C(13)–C(19)			127(1)	124.1(5)
C(13)–C(19)–C(18)				129.7(5)
C(21)–C(20)–C(26)				123.6(5)
C(20)–C(21)–C(22)				122.1(5)
C(21)–C(22)–C(23)				122.0(5)
C(24)–C(23)–C(22)				113.6(5)
C(23)–C(24)–C(25)				113.3(5)
C(26)–C(25)–C(24)				124.8(5)
C(25)–C(26)–C(20)				122.6(6)

Solid-state structures of $[Ru_6C(CO)_{15}(ENBD)]$ 1, $[Ru_6C(CO)_{14}(C_7H_8)]$ 2 and $[Ru_6C(CO)_{11}(\eta^5\text{-}C_7H_9)(\mu_3\text{-}\eta^2:\eta^2:\eta^3\text{-}C_7H_7)]$ 3

The molecular structures of clusters **1**, **2** and **3** are closely related and will be described together. Schematic representations of the solid-state molecular structures together with labelling schemes are given in Figs. 1 and 2 for the two independent molecules of compound **1**, and in Figs. 3 and 5 for compounds **2** and **3**, respectively. Relevant bond distances and angles are reported in Tables 1, 2 and 3. All three compounds belong to the family of derivatives of $[Ru_6C(CO)_{17}]$[8] and bear many similarities to mono- and bis-arene clusters of the type $[Ru_6C(CO)_{14}(\eta^6\text{-arene})]$ and $[Ru_6C(CO)_{11}(\eta^6\text{-arene})(\mu_3\text{-}\eta^2:\eta^2:\eta^2\text{-arene})]$ (arene = benzene, toluene, mesitylene, xylene, *etc.*).[1] In all cases, the metal-atom framework constitutes an octahedron of Ru atoms encapsulating a C (carbide) atom.

Compound **1** possesses fifteen CO ligands and carries the ethylenenorbornadiene (ENBD) ligand in an apical position interacting with one Ru-atom in η^4-fashion (see Figs. 1 and 2). The ENBD ligand formally replaces two CO ligands from the parent $[Ru_6C(CO)_{17}]$.[8] Contrary to observations made on other substituted derivatives of $[Ru_6C(CO)_{17}]$, the two bridging CO ligands span two consecutive edges of the octahedral cluster with the participation of the atom carrying the ENBD ligand. The other more general behaviour is for the two bridging ligands to span the equatorial plane which does not include the hetero-ligand.

The reason for this change may be found from a consideration of the fifteenth CO [C(11)] carried by the Ru atom involved in the ENBD bonding. This CO ligand is 'pushed' towards a bridging position by the adjacent organo-ligand.

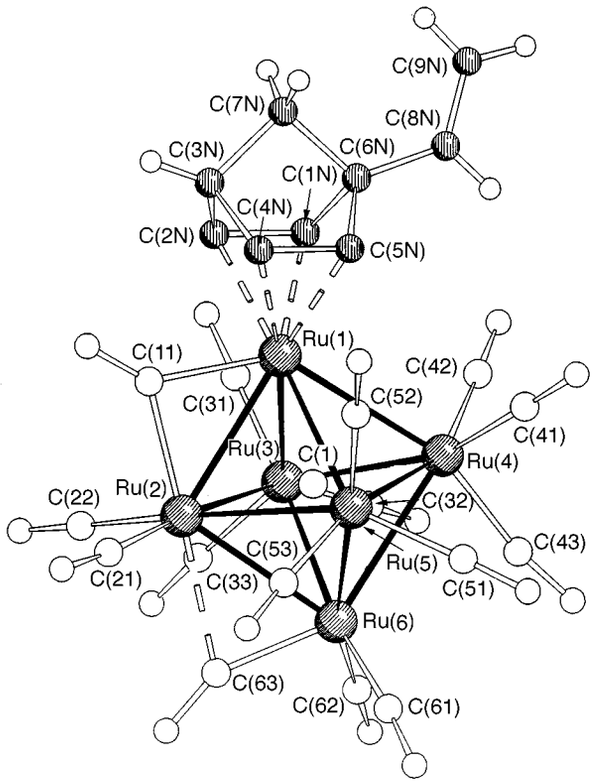

Fig. 1 The molecular structure of cluster **1a** in the solid state

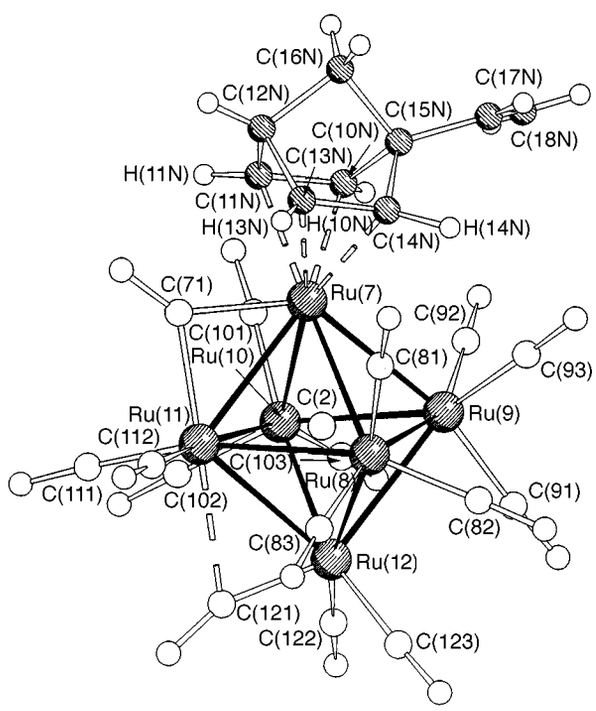

Fig. 2 The molecular structure of cluster **1b** in the solid state. Note the different orientation of the ethylene group with respect to molecule **1a**. Hydrogen atoms bound to the C atoms interacting with the cluster were directly located from Fourier maps

Furthermore, ENBD is almost certainly a poorer π-acceptor than CO, *i.e.* the Ru atom Ru(1) is electron-rich and needs to delocalise the additional electron density over its neighbouring atom *via* the CO bridge. The same CO ligand distribution is present in the second independent molecule of **1**.

The major structural difference between the two molecules resides in the orientation of the ethylene tail which differs by a 90° rotation in the two structures which crystallize as two independent molecules. The relatively good quality of the diffraction data for **1** allowed location of the ENBD hydrogen atoms in one of the two molecules (molecule **1b**, see Fig. 2) whereas H atoms in molecule **1a** had to be placed in calculated positions. The C–H bonds are bent away from the Ru atom deviating slightly from the plane of co-ordination of the C=C double bonds. This is in keeping with the general behaviour of metal co-ordinated unsaturated olefins or carbocycles. Average Ru–C distances are 2.198(12) and 2.188(12) Å for **1a** and **1b**, respectively, and the effect of co-ordination is shown in the average C=C distances of 1.41(2) and 1.41(2) Å.

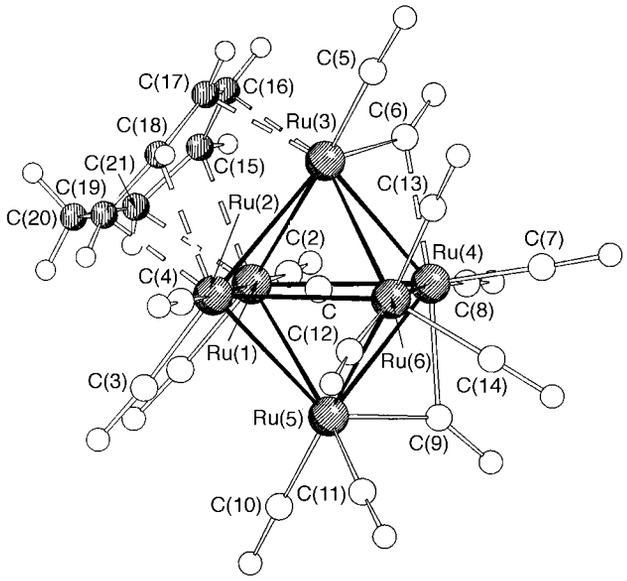

Fig. 3 The molecular structure of cluster **2** in the solid state showing the labelling scheme

Compounds **2** and **3** provide an example of the co-ordinative variability of carbocyclic rings based on the C_7-frame. Indeed, while **2** bears a facially bound C_7H_8 ligand, *viz.* co-ordinated as μ_3-η^2:η^2:η^2, compound **3** carries a terminally bound η^5-C_7H_9 ligand and a facially co-ordinated μ_3-η^2:η^2:η^3-C_7H_7 ligand. The three ligands C_7H_7, C_7H_8 and C_7H_9, can therefore, depending on the degree of unsaturation, adopt themselves to the electronic requirements of the cluster frame by formally donating seven-, six- and five-electrons, respectively. It is worth stressing that the quality of the X-ray data was sufficient to allow the location of hydrogen atom positions from the Fourier maps.

The structure of cluster **2** is reminiscent of that of many arene clusters of ruthenium carrying facially bound ligands. Although cluster species of the type $[Ru_6C(CO)_{14}(\eta^6\text{-}C_6H_6)]$,[10] $[Ru_6C(CO)_{11}(\eta^6\text{-}C_6H_6)(\mu_3\text{-}C_6H_6)]$[11] and $[Ru_6C(CO)_{11}(\eta^6\text{-}C_6H_6)_2]$[12] are known, it has never been possible to isolate the mono-benzene derivative $[Ru_6C(CO)_{14}(\mu_3\text{-}C_6H_6)]$ with benzene bound facially. Cluster **2** provides an example of a compound isoelectronic with this latter structure. In **2** the CO ligands are distributed, twelve terminally bound and two in a semibridging position (see Fig. 3). The carbocyclic ligand is placed almost parallel to a cluster triangular face with the CH_2 group accommodated between two terminal CO's. A projection perpendicular to the triangle plane is shown in Fig. 4(a), whereas a side view is shown in Fig. 4(b). The two drawings show the co-ordination geometry in detail with one C–C bond perfectly overlapping atom Ru(3) and the other two slightly off-center over Ru(1) and Ru(2). The C–C bond distance distributions are indicative, within the degree of accuracy of the data, of delocalization over the six C atoms interacting with the cluster face, while C–C bonds involving the CH_2 groups are markedly longer and indicative of single bond order (see Table 1).

As mentioned above the two carbocyclic ligands in **3** provide an odd number of electrons, *i.e.* five and seven, respectively. The apical ligand (see Fig. 5) has a chair-like conformation with a

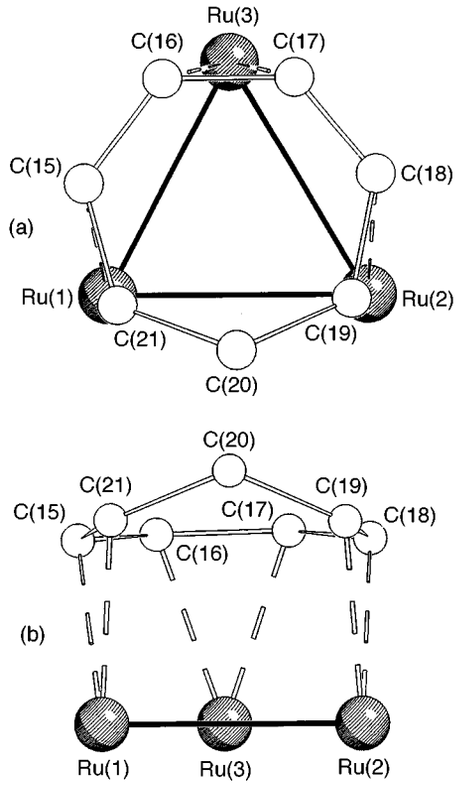

Fig. 4 (a) Projection perpendicular to the triangle plane in cluster **2**, (b) side view of cluster **2**

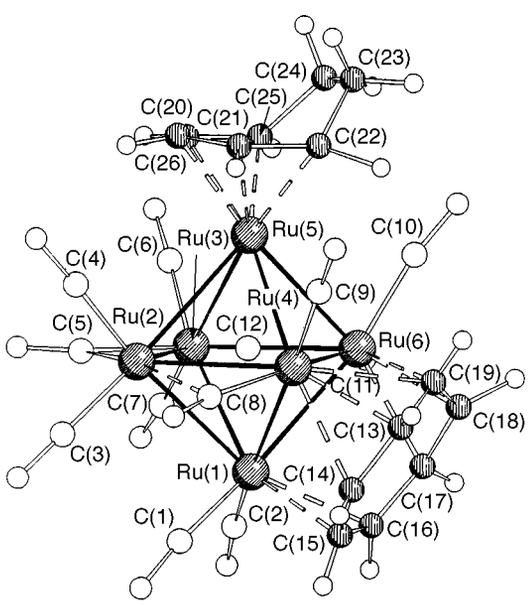

Fig. 5 The molecular structure of cluster **3** in the solid state showing the labelling scheme

flat C_5 system interacting with the apex Ru(5), and of a bent C_2H_4 unit. The electron delocalization involves all five atoms [Ru–C distance range is 2.153(5)–2.221(5) Å]. The second C_7H_7 ligand is flat and parallel to the triangular face not involving the apical atom carrying the C_7H_9 ligand. The geometry of coordination is fully reminiscent of benzene face-capping. Hydrogen atoms are slightly bent out of the plane of the ligand. A projection perpendicular to the ligand plane is shown in Fig. 6. The CO ligand distribution is the same as that generally observed with bis-arene clusters carrying apical and facial ligands simultaneously. We find suggestive that $[Ru_6C(CO)_{11}(\eta^5\text{-}C_7H_9)(\mu_3\text{-}\eta^2:\eta^2:\eta^3\text{-}C_7H_7)]$ is isoelectronic and almost isostructural with $[Ru_6C(CO)_{11}(\eta^6\text{-}C_6H_6)(\mu_3\text{-}\eta^2:\eta^2:\eta^2\text{-}C_6H_6)]$

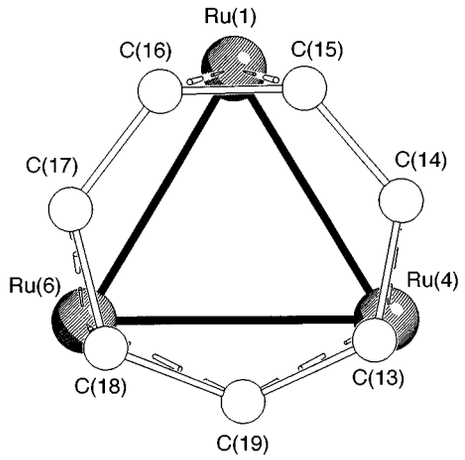

Fig. 6 Projection perpendicular to the ligand plane in cluster **3**

because the facial ligand provides the extra electron that is missing from the interaction with the apical ligand. The C–C bond length distribution within the facial ligand indicates full electron delocalization.

Conclusion

In this work we have explored the chemistry of the cluster $[Ru_6C(CO)_{17}]$ with cycloheptatriene. Again, we have been able to observe the change in the C_7 skeleton from the monocyclic C_7 unit through the bicyclic norbornene unit and finally to toluene. This observation is totally in accord with those made on the Pt(111) (and other) surface.

Experimental

All reactions were carried out with exclusion of air under an atmosphere of dried nitrogen, using freshly distilled solvents. Product separation was achieved by thin layer chromatography (TLC) using glass plates supplied by Merck, pre-coated with a 0.25 mm layer of Kieselgel $60F_{254}$. Eluents were mixed from standard laboratory grade solvents. Infrared spectra were recorded using NaCl cells (0.5 mm path length) on a Perkin-Elmer 1710 Series Fourier-transform spectrometer, calibrated with carbon dioxide. Fast atom bombardment (FAB) mass spectra were obtained on a Kratos MS50TC spectrometer. The instrument was run in positive mode, using CsI as calibrant. Proton NMR spectra were recorded in $CDCl_3$ on Bruker WH200 Fourier-transform spectrometers, all chemical shifts being reported relative to internal $SiMe_4$. The cluster $[Ru_6C(CO)_{17}]$ was prepared according to the literature methods.[8] Cycloheptatriene was purchased from Aldrich chemicals. For all molecular representation the graphic program SCHAKAL 92[13] was used.

Synthesis of $[Ru_6C(CO)_{15}(ENBD)]$ 1, $[Ru_6C(CO)_{14}(C_7H_8)]$ 2 and $[Ru_6C(CO)_{11}(C_7H_9)(C_7H_7)]$ 3

The cluster $[Ru_6C(CO)_{17}]$ (150 mg) and cycloheptatriene (0.3 ml) were dissolved in dry octane (50 ml) and heated to reflux for 18 h. The reaction mixture turned brown in colour. The solvent was removed under reduced pressure and the residue dissolved in a minimum amount of CH_2Cl_2 and the products purified by TLC on silica plates using CH_2Cl_2–hexane (3:7, v/v) as the eluent. Four of these products were identified as the previously characterized compounds $[Ru_6C(CO)_{14}(\eta^6\text{-}C_6H_5CH_3)]$ **4** (10%), $[Ru_6C(CO)_{15}(ENBD)]$ **1** (30%), $[Ru_6C(CO)_{14}(C_7H_8)]$ **2** (10%) and $[Ru_6C(CO)_{11}(C_7H_9)(C_7H_7)]$ **3** (15%).

Spectroscopic data

Spectroscopic data for cluster 1. IR $\nu_{CO}(CH_2Cl_2)$: 2053vs,

Table 4 Crystal data and details of measurements for crystals of clusters **1a**, **1b**, **2** and **3**

	1a, **1b**	**2**	**3**
Formula	$C_{25}H_{10}O_{15}Ru_6$	$C_{22}H_8O_{14}Ru_6 \cdot 0.5CH_2Cl_2$	$C_{26}H_{16}O_{11}Ru_6$
M	1154.73	1145.45	1110.81
T/K	223(2)	293(2)	293(2)
System	Monoclinic	Monoclinic	Monoclinic
Space group	$P2_1/n$	$P2_1/c$	$C2/c$
Z	8	4	8
a/Å	16.982(4)	18.216(9)	15.566(8)
b/Å	17.729(5)	8.965(4)	12.060(7)
c/Å	21.017(5)	18.414(7)	29.87(3)
β/°	107.56(2)	109.16(4)	94.64(6)
U/Å^3	6033(3)	2841(2)	5588(7)
F(000)	4336	2148	4192
λ(Mo-Kα)/Å	0.710 73	0.710 73	0.710 73
μ(Mo-Kα)/mm^{-1}	3.000	3.369	3.222
θ Range/°	2.5–25.0	2.5–25.0	3.0–25.0
ψ Scan correction, minimum, maximum transmission	0.91, 1.00	0.82, 1.00	0.88, 1.00
Octants explored	$0 \leqslant h \leqslant 20$, $0 \leqslant k \leqslant 21$, $-24 \leqslant l \leqslant 23$	$-21 \leqslant h \leqslant 21$, $0 \leqslant k \leqslant 10$, $0 \leqslant l \leqslant 21$	$-18 \leqslant h \leqslant 18$, $0 \leqslant k \leqslant 14$, $0 \leqslant l \leqslant 35$
Measured reflections	10 950	5157	5017
Unique reflections	10 568	4984	4910
No. refined parameters	739	383	388
Goodness of fit on F^2	1.050	0.918	1.109
$R1$[on F, $I > 2\sigma(I)$]	0.0535	0.0437	0.0200
w$R2$(on F^2, all data)	0.1348	0.1411	0.0566

2035vs, 2083w, 2067vw (sh), 1992w (sh), 1825w (br) cm^{-1}. FAB mass spectrum (M^+): 1156 (obs.), 1156 (calc.). ^{1}H NMR ($CDCl_3$): δ 6.30–6.38 (q), 5.36–5.40 (q), 4.12 (s), 3.72 (t), 3.57 (d).

Spectroscopic data for cluster 2. IR $\nu_{CO}(CH_2Cl_2)$: 2076w, 2039vs, 2026vs, 1819w (br) cm^{-1}. ^{1}H NMR ($CDCl_3$): δ 5.70 (m), 3.61 (m).

Spectroscopic data for cluster 3. IR $\nu_{CO}(CH_2Cl_2)$: 2070vw, 2040m, 2005vs, 1954w (sh), 1797w (br) cm^{-1}. FAB mass spectrum (M^+): 1112 (obs.), 1110 (calc.). ^{1}H NMR ($CDCl_3$): δ 7.71 (m), 7.52 (m), 6.00 (m), 4.90 (m), 4.30 (m), 4.10 (m).

Crystallography

The computer programs SHELX 86[14] and SHELXL 93[15] were used for structure solution and refinement.

Structural data for cluster 1. (See Table 4.) All atoms except the hydrogen atoms were treated anisotropically; H atoms, with the exception of H(10), H(11), H(13) and H(14), were added in calculated positions (C–H 1.08 Å), whilst these latter hydrogens were located directly from the final low θ (<20°) Fourier maps.

Structural data for cluster 2. (See Table 4.) All atoms except the hydrogen atoms were treated anisotropically; H atoms were added in calculated positions (C–H 1.08 Å).

Structural data for cluster 3. (See Table 4.) All atoms except the hydrogen atoms were treated anisotropically; H atoms were located directly from final low θ (<20°) Fourier maps.

CCDC reference number 186/894.

Acknowledgements

We thank the EU for their support through Training and Mobility of Researchers, and NATO for financial support. F. G. thanks the RSC for an International Author Grant.

References

1 D. Braga, P. J. Dyson, F. Grepioni and B. F. G. Johnson, *Chem. Rev.*, 1994, **94**, 1585.
2 E. L. Muetterties and S. T. Olin, *Bull. Soc. Chim. Belg.*, 1975, **84**, 959.
3 E. L. Muetterties, *Science*, 1977, **196**, 839.
4 J. F. Roth, J. H. Craddock, A. Hershman and F. E. Paulik, *Chem. Technol.*, October 1971, 600; *Chem. Eng. News*, 26 April 1971, 30.
5 R. Gomer (Editor), *Topics in Applied Physics*, Springer-Verlag, New York, 1975, vol. 4.
6 M. C. Tsai, C. M. Friend and E. L. Muetterties, *J. Am. Chem. Soc.*, 1982, **104**, 2539; M. E. Bussel, F. C. Henn and C. T. Campbell, *J. Phys. Chem.*, 1992, **96**, 5978; F. C. Henn, A. L. Diaz, M. E. Domagala and C. T. Campbell, *J. Phys. Chem.*, 1992, **96**, 5965; M. B. Hugenschmidt, A. L. Diaz and C. T. Campbell, *J. Phys. Chem.*, 1992, **96**, 5974.
7 D. B. Brown, P. J. Dyson, B. F. G. Johnson, C. M. Martin, D. Parker and S. Parsons, *J. Chem. Soc., Dalton Trans.*, in the press.
8 A. Sirigu, M. Bianchi and E. Benedetti, *Chem. Commun.*, 1969, 596; D. Braga, F. Grepioni, P. Dyson, B. F. G. Johnson, P. Frediani, M. Bianchi and F. Piacenti, *J. Chem. Soc., Dalton Trans.*, 1992, 2565.
9 L. Farrugia, *Acta Crystallogr., Sect. C*, 1988, **44**, 997.
10 D. Braga, F. Grepioni, B. F. G. Johnson, H. Chen and J. Lewis, *J. Chem. Soc., Dalton Trans.*, 1991, 2559.
11 R. D. Adams and W. Wu, *Polyhedron*, 1992, 2121.
12 M. P. Gomez-Sal, B. F. G. Johnson, J. Lewis, P. R. Raithby and A. H. Wright, *J. Chem. Soc., Chem. Commun.*, 1985, 1682.
13 E. Keller, SCHAKAL 93, Graphical Representation of Molecular Models, University of Freiburg, 1993.
14 G. M. Sheldrick, *Acta Crystallogr., Sect. A*, 1990, **46**, 467.
15 G. M. Sheldrick, SHELX 92, Program for Crystal Structure Determination, University of Göttingen, 1993.

Received 2*nd January* 1998; *Paper* 8/00010G